Traffic Density Estimation with the Cell Transmission Model[1]

Laura Muñoz, Xiaotian Sun, Roberto Horowitz[2], Luis Alvarez[3]
Department of Mechanical Engineering
University of California at Berkeley
Berkeley, CA 94720-1740

Abstract

A macroscopic traffic flow model, called the switching-mode model (SMM), has been derived from the cell transmission model (CTM) and then applied to the estimation of traffic densities at unmonitored locations along a highway. The SMM is a hybrid system that switches among different sets of linear difference equations, or modes, depending on the mainline boundary data and the congestion status of the cells in a highway section. Using standard linear systems techniques, the observability and controllability properties of the SMM modes have been determined. Both the SMM and a density-based version of the CTM have been simulated over a section of I-210 West in Southern California, using several days of loop detector data collected during the morning rush-hour period. The simulation results show that the SMM and CTM produce density estimates that are both similar to one another and in good agreement with measured densities on I-210. The mean percentage error averaged over all the test days was approximately 13% for both models.

1 Introduction

Freeway traffic data is often available in the form of occupancy and volume measurements collected from single or double loop detectors embedded in the pavement [1]. In conjunction with effective vehicle length data, these measurements can be converted into macroscopic quantities such as traffic density and speed. Loop detector data sets are often incomplete or contain bad samples. For instance, from [1] it can be seen that approximately 30% of the possible loop samples in California's District 7, which contains over 30 freeways, were missing, on average, over the period from March 2002 to February 2003. However, on-ramp metering control strategies, such as ALINEA [2], require accurate local traffic density information in order to effectively regulate on-ramp inflows to the freeway. It is thus essential to have a means of reconstructing missing traffic density measurements.

To address these concerns, an open-loop density estimator, based on the cell transmission model (CTM) [3, 4], has been designed, and has been shown to perform well when tested with data from Interstate 210 in Southern California. We refer to this estimator as the *switching-mode model* (SMM). The switching-mode model is a linear time-varying model, derived from a *modified cell transmission model* that uses density instead of occupancy as its state variable.

The cell transmission model, a macroscopic traffic model, was selected for this research due to its analytical simplicity and ability to reproduce congestion wave propagation dynamics. The CTM has previously been validated for a single freeway link (with no on-ramps or off-ramps) using data from I-880 in California [5]. The modified CTM, from which the SMM is derived, is similar to that of [3, 4], except that it (1) uses cell densities as state variables instead of cell occupancies, (2) accepts nonuniform cell lengths, and (3) allows congested conditions to be maintained at the downstream boundary of a modeled freeway section.

Using cell densities instead of cell occupancies permits the CTM to to include uneven cell lengths, which leads to greater flexibility in partitioning the highway. Nonuniform cell lengths also enable us to use a smaller number of cells to describe a given highway segment, thus reducing the size of the state vector $[\rho_1 \dots \rho_N]^T$, where ρ_i is the density of the i^{th} cell. While it is expected that partitioning a segment into a large number of cells can improve numerical accuracy, our interest here is to test our methods using a smaller state vector and to simplify the design of estimators and controllers. Allowing congested flow rates at downstream boundaries is necessary to enable the model to work with real highway data.

In the modified CTM, a highway is partitioned into a series of cells. The density of cell i evolves according to conservation of vehicles. For the case of a linear highway segment with no on- or off-ramps, vehicle conservation can be written as

$$\rho_i(k+1) = \rho_i(k) + \tfrac{T_s}{l_i}(q_i(k) - q_{i+1}(k)). \qquad (1)$$

Here, k is the time index, T_s is the discrete time interval, l_i is the length of cell i, and $q_i(k)$ is the flow rate, in vehicles per unit time, into cell i during the interval $[k,\ k+1)$. As described in [4], $q_i(k)$ is determined by taking the minimum of two quantities:

$$q_i(k) = \min(S_{i-1}(k), R_i(k)), \qquad (2)$$

where $S_{i-1}(k) = \min(v\rho_{i-1}(k), Q_{M,i-1})$, is the maxi-

[1]Research supported by UCB-ITS PATH grant TO 4136
[2]Professor, horowitz@me.berkeley.edu; author for correspondence.
[3]Professor, Universidad Nacional Autónoma de México.

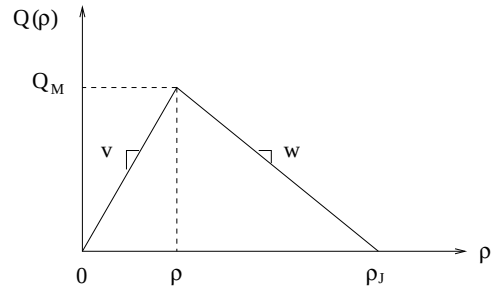

Figure 1: Flow as a function of density

mum flow that can be *supplied* by cell $i-1$ under free-flow conditions, over the interval $[k,\ k+1)$, and $R_i(k) = \min(Q_{M,i}, w(\rho_J - \rho_i(k)))$, is the maximum flow that can be *received* by cell i under congested conditions, over the same time interval. Eqs. (1) and (2) are the density-based equivalents of those described in [3]. The modified CTM also uses density-based versions of the merge and diverge laws of [4] to incorporate on-ramp and off-ramp flows.

The CTM parameters are depicted in the fundamental diagram of Fig. 1. They can be valid for all cells or allowed to vary for each cell. The free-flow speed v is the average speed at which vehicles travel down the highway under uncongested (low density) conditions. w is the average speed at which congestion waves propagate upstream through the highway under fully congested conditions. Q_M is the maximum flow that occurs at critical density ρ_c, and ρ_J is the jam density.

It is helpful to review here some of the terminology and naming conventions that will be used throughout this paper. The *congestion status* of cell i is determined by comparing the cell density with the critical density: if $\rho_i < \rho_{c,i}$, the cell has free-flow status, otherwise $\rho_i \geq \rho_{c,i}$ and the cell has congested status. The SMM switches between several sets of linear difference equations depending on the values of the mainline boundary inputs and on the congestion status of the cells in a section. Each set of linear equations is referred to as a *mode* of the SMM. The SMM estimates the movement of congestion *wave fronts* through a highway section. Here, a wave front is understood to be a status transition, upstream of which nearby cells have one status (e.g. free-flow), and downstream of which nearby cells have the opposite status.

2 Switching-Mode Model

In the switching-mode model, we describe the cell transmission model as a hybrid system that switches between 5 sets of linear difference equations, depending on the congestion status of the cells and the values of the mainline boundary data. Assuming our state variable is the cell densities, $\boldsymbol{\rho} = [\rho_1 \dots \rho_N]^T$, the key difference between the CTM and the SMM is that, with respect to density, the former is nonlinear, whereas each mode of the latter is linear. The SMM can be extracted from the modified CTM by writing each inter-cellular flow, q_i, as either an explicit function of cell density, $v\rho_{i-1}(k)$ or $w(\rho_J - \rho_i(k))$, or as a constant, Q_M. This explicit density dependence is achieved by supplying a set of logical rules that determine the congestion status of each cell, at every time step, based on measurements at the segment boundaries.

For simplicity, the following assumptions are made:

1. The densities and flows at the upstream and downstream segment boundaries, as well as flows on all the on-ramps and off-ramps, are measured.
2. There is at most one status transition (or wave front) in the highway section. If both the upstream and downstream mainline boundaries are of the same status, i.e., both free-flow or both congested, we assume that all the mainline cells, 1 through N, have the same status; while if the two boundaries are of different status, there exists a single wave front in the segment, upstream of which all the cells have congested (free-flow) status, and downstream of which all cells have free-flow (congested) status.

The single-wave front assumption is an approximation that is expected to be acceptable for short highway segments with only one on-ramp and off-ramp, such as the example later in this section. To more accurately deal with longer sections with many on- and off-ramps, the switching logic can be modified to allow multiple wave fronts within a segment.

Since an SMM-modeled section contains at most one congestion wave front, the modes of the SMM can be distinguished by the congestion status of the cells upstream and downstream of the wave front. If there is no wave front in the section, we can use a doubled label, e.g."Free-flow–Free-flow" to indicate the absence of any status transition. The five modes are denoted: (1) "Free-flow–Free-flow" (FF), (2) "Congestion–Congestion" (CC), (3) "Congestion–Free-flow" (CF), (4) "Free-flow–Congestion 1" (FC1), and (5) "Free-flow–Congestion 2" (FC2). The two modes of "Free-flow–Congestion" are determined by the relative magnitudes of the *supplied* flow of the last uncongested cell upstream of the wave front and the *receiving* flow of the the first congested cell downstream of the wave front. If the former is larger, the SMM is in FC1; while if the latter is larger, it is in FC2. Respectively, these two cases are distinguished by whether the congestion wave is traveling backward or forward within the segment.

Consider the highway segment in Fig. 2, which is divided into 4 cells. The measured aggregate flows and densities at the upstream and downstream mainline detectors are denoted by q_u, ρ_u, and q_d, ρ_d. All five modes of the SMM can be summarized as follows:

$$\boldsymbol{\rho}(k+1) = A_s\ \boldsymbol{\rho}(k) + B_s\ \boldsymbol{u}(k) + B_{J,s}\ \boldsymbol{\rho}_J + B_{Q,s}\ \boldsymbol{q}_M, \quad (3)$$

Proceedings of the American Control Conference
Denver, Colorado June 4-6, 2003

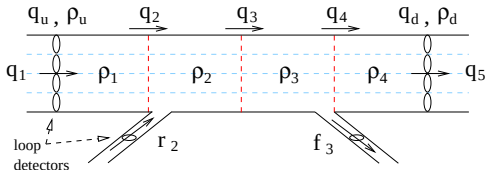

Figure 2: Highway segment divided into 4 cells

where $s = 1, 2, 3, 4, 5$ indicates the mode (1: FF, 2: CC, 3: CF, 4: FC1, 5: FC2), $\boldsymbol{\rho} = [\rho_1 \dots \rho_4]^T$ is the state, and $\boldsymbol{u} = [q_u \;\; r_2 \;\; f_3 \;\; \rho_d]^T$ are the flow and density inputs; specifically, r_2 and f_3 are the measured on-ramp and off-ramp flows entering and leaving the section, subscripted according to their cell of entry or exit. $\boldsymbol{\rho}_J = [\rho_{J1} \;\; \rho_{J2} \;\; \rho_{J3} \;\; \rho_{J4} \;\; \rho_{J5}]^T$ is the vector of jam densities, and $\boldsymbol{q}_M = [Q_{M1} \;\; Q_{M2} \;\; Q_{M3} \;\; Q_{M4}]^T$ is the vector of maximum flow rates.

In the FF mode, each cell is able to accept the flow supplied by its upstream neighboring cell; and cell 1 accepts all of the boundary inflow q_u, while cell 4 dumps vehicles at the free-flow speed v_4. The state matrices are

$$A_1 = \begin{bmatrix} 1-\frac{v_1T_s}{l_1} & 0 & 0 & 0 \\ \frac{v_1T_s}{l_2} & 1-\frac{v_2T_s}{l_2} & 0 & 0 \\ 0 & \frac{v_2T_s}{l_3} & 1-\frac{v_3T_s}{l_3} & 0 \\ 0 & 0 & \frac{v_3T_s}{l_4} & 1-\frac{v_4T_s}{l_4} \end{bmatrix},$$

$$B_1 = \begin{bmatrix} \frac{T_s}{l_1} & 0 & 0 & 0 \\ 0 & \frac{T_s}{l_2} & 0 & 0 \\ 0 & 0 & 0 & -\frac{T_s}{l_4} \\ 0 & 0 & 0 & 0 \end{bmatrix},$$

$$B_{J,1} = 0_{4\times 5}, \quad B_{Q,1} = 0_{4\times 4}. \tag{4}$$

In the CC mode, each cell can only dump the amount of flow that can be accepted by the downstream neighboring cell. The number of vehicles that cell 4 can emit is determined by the boundary density ρ_d, while cell 4 receives vehicles up to its capacity. The state matrices are

$$A_2 = \begin{bmatrix} 1-\frac{w_1T_s}{l_1} & \frac{w_2T_s}{l_1} & 0 & 0 \\ 0 & 1-\frac{w_2T_s}{l_2} & \frac{w_3T_s}{l_2} & 0 \\ 0 & 0 & 1-\frac{w_3T_s}{l_3} & \frac{w_4T_s}{l_3} \\ 0 & 0 & 0 & 1-\frac{w_4T_s}{l_4} \end{bmatrix},$$

$$B_2 = \begin{bmatrix} 0 & \frac{T_s}{l_1} & 0 & 0 \\ 0 & 0 & 0 & 0 \\ 0 & 0 & -\frac{T_s}{l_3} & 0 \\ 0 & 0 & 0 & \frac{w_5T_s}{l_4} \end{bmatrix},$$

$$B_{J,2} = \begin{bmatrix} \frac{w_1T_s}{l_1} & -\frac{w_2T_s}{l_1} & 0 & 0 & 0 \\ 0 & \frac{w_2T_s}{l_2} & -\frac{w_3T_s}{l_2} & 0 & 0 \\ 0 & 0 & \frac{w_3T_s}{l_3} & -\frac{w_4T_s}{l_3} & 0 \\ 0 & 0 & 0 & \frac{w_4T_s}{l_4} & -\frac{w_5T_s}{l_4} \end{bmatrix},$$

$$B_{Q,2} = 0_{4\times 4}. \tag{5}$$

In the CF mode, there exists one congestion-to-free-flow transition inside the section. One property of the SMM is that the wave front will always lie on a cell boundary. Cells upstream of the wave front behave as congested cells, while cells downstream of the wave front release vehicles at the free-flow rate. The wave front itself acts as a bottleneck, expelling vehicles at maximum allowed rate Q_M, and decoupling the region upstream of the wave front from the downstream region. For the case where the wave front is located in between cells 2 and 3, the state matrices are:

$$A_3 = \begin{bmatrix} 1-\frac{w_1T_s}{l_1} & \frac{w_2T_s}{l_1} & 0 & 0 \\ 0 & 1-\frac{w_2T_s}{l_2} & 0 & 0 \\ 0 & 0 & 1-\frac{v_3T_s}{l_3} & 0 \\ 0 & 0 & \frac{v_3T_s}{l_4} & 1-\frac{v_4T_s}{l_4} \end{bmatrix},$$

$$B_3 = \begin{bmatrix} 0 & \frac{T_s}{l_1} & 0 & 0 \\ 0 & 0 & 0 & 0 \\ 0 & 0 & -\frac{T_s}{l_3} & 0 \\ 0 & 0 & 0 & 0 \end{bmatrix},$$

$$B_{J,3} = \begin{bmatrix} \frac{w_1T_s}{l_1} & -\frac{w_2T_s}{l_1} & 0 & 0 & 0 \\ 0 & \frac{w_2T_s}{l_2} & 0 & 0 & 0 \\ 0 & 0 & 0 & 0 & 0 \\ 0 & 0 & 0 & 0 & 0 \end{bmatrix},$$

$$B_{Q,3} = \begin{bmatrix} 0 & 0 & 0 & 0 \\ 0 & 0 & -\frac{T_s}{l_2} & 0 \\ 0 & 0 & \frac{T_s}{l_3} & 0 \\ 0 & 0 & 0 & 0 \end{bmatrix}. \tag{6}$$

In both FC modes, one free-flow-to-congestion transition exists inside the section. Unlike the previous mode, the state matrices change depending on the direction of motion of the wave front. In FC1, the wave front moves downstream. Assuming, for example, that the wave front is between cells 2 and 3, the state matrices for this mode are:

$$A_4 = \begin{bmatrix} 1-\frac{v_1T_s}{l_1} & 0 & 0 & 0 \\ \frac{v_1T_s}{l_2} & 1-\frac{v_2T_s}{l_2} & 0 & 0 \\ 0 & \frac{vT_s}{l_3} & 1 & \frac{w_4T_s}{l_3} \\ 0 & 0 & 0 & 1-\frac{w_4T_s}{l_4} \end{bmatrix},$$

$$B_4 = \begin{bmatrix} \frac{T_s}{l_1} & 0 & 0 & 0 \\ 0 & \frac{T_s}{l_2} & 0 & 0 \\ 0 & 0 & -\frac{T_s}{l_3} & 0 \\ 0 & 0 & 0 & \frac{w_5T_s}{l_4} \end{bmatrix},$$

$$B_{J,4} = \begin{bmatrix} 0 & 0 & 0 & 0 & 0 \\ 0 & 0 & 0 & 0 & 0 \\ 0 & 0 & 0 & -\frac{w_4T_s}{l_3} & 0 \\ 0 & 0 & 0 & \frac{w_4T_s}{l_4} & -\frac{w_5T_s}{l_4} \end{bmatrix},$$

$$B_{Q,4} = 0_{4\times 4}. \tag{7}$$

For FC2, the wave moves upstream. Again assuming that the wave front is between cells 2 and 3, this mode differs from the previous case in that, due to the dominance of the congested flow rate at the wave front boundary, the tridiagonal row is now the second instead of the third row, and more terms appear in $B_{J,s}$:

$$A_5 = \begin{bmatrix} 1-\frac{v_1T_s}{l_1} & 0 & 0 & 0 \\ \frac{v_1T_s}{l_2} & 1 & \frac{w_4T_s}{l_2} & 0 \\ 0 & 0 & 1-\frac{w_3T_s}{l_3} & \frac{w_4T_s}{l_3} \\ 0 & 0 & 0 & 1-\frac{w_4T_s}{l_4} \end{bmatrix},$$

$$B_5 = B_4,$$

$$B_{J,5} = \begin{bmatrix} 0 & 0 & 0 & 0 & 0 \\ 0 & 0 & -\frac{w_3 T_s}{l_2} & 0 & 0 \\ 0 & 0 & \frac{w_3 T_s}{l_3} & -\frac{w_4 T_s}{l_3} & 0 \\ 0 & 0 & 0 & \frac{w_4 T_s}{l_4} & -\frac{w_5 T_s}{l_4} \end{bmatrix},$$

$$B_{Q,5} = 0_{4\times 4}. \tag{8}$$

At each time step, the SMM determines its mode based on the measured mainline boundary data and the congestion status of the cells in the section. If both ρ_u and ρ_d have free-flow status, the FF mode is selected, and if both of these densities are congested, the CC mode is selected. If ρ_u and ρ_d are of opposite status, then the SMM performs a search over the ρ_i to determine whether there is a status transition inside the section. This wave front search consists of searching through the cells, in order, looking for the first status transition between adjacent cells. It is expected that some error will be induced in the wave front location predicted by the SMM, since the search for a status transition is performed on the states estimated by the SMM, and not the actual, unmeasured state. A stochastic estimation method, based on the SMM, that uses output feedback to correct both estimated densities and predicted wave front locations, has been developed and will be documented in an upcoming PATH report.

2.1 General results on observability

Table 1 summarizes the observability for each SMM mode. The observability results were derived using standard linear systems techniques. On the left side, "upstream cells" and "downstream cells" give the status of cells both upstream and downstream of the congestion wave front. If there is no such wave front, both sets of cells have the same status. The right side indicates which of the two mainline boundary measurements, if either, can be used to make the SMM observable. To relate the measurements to the states, in Fig. 2, it is assumed that ρ_u is a measurement of ρ_1 and ρ_d is a measurement of ρ_4.

These results can be obtained by computing the observability matrices for the A_s of Eq. (3) with the output matrices $C_u = [1\ 0\ 0\ 0]$ and $C_d = [0\ 0\ 0\ 1]$, or with the combined output matrix $C = \begin{bmatrix} C_u^T & C_d^T \end{bmatrix}^T$. For example, for the FF mode, it can be shown that (A_1, C_u) is not observable, whereas (A_1, C_d) is. From the table, it can be seen, as a general result, that if all cells have free-flow status, the states are observable using a downstream measurement, while in congested mode, they are observable using an upstream measurement. If there is no downstream measurement available when cells are in free-flow mode, or there is no upstream measurement when cells are congested, as in the last two cases listed in Table 1, the system is unobservable. This is related to the wave (information) propagation directions on a highway in different congestion modes. When a highway section is in free-flow mode, the information propagates downstream at speed v, which is the vehicle traveling speed. Therefore, in order to be able to estimate the cell densities, the downstream density measurement is needed. When the highway is in congestion, the information propagates upstream at speed w, which is the backward congestion wave traveling speed, and an upstream measurement is needed to estimate densities.

Table 1: Observability for different SMM modes

Upstr. Cells	Downstr. Cells	Observable with
Free-flow	Free-flow	Downstr. Meas.
Congested	Congested	Upstr. Meas.
Congested	Free-flow	Up. and Down. Meas.
Free-flow	Congested 1	Unobservable
Free-flow	Congested 2	Unobservable

Table 2: Controllability for different SMM modes

Upstr. Cells	Downstr. Cells	Controllable from
Free-flow	Free-flow	Upstr. On-Ramp
Congested	Congested	Downstr. On-Ramp
Congested	Free-flow	Not Controllable
Free-flow	Congested 1	Up. and Down. O.R.
Free-flow	Congested 2	Up. and Down. O.R.

2.2 General results on controllability

Controllability results are summarized in Table 2. These results can be derived in a similar manner as the observability results; e.g., for the FF mode, if A_1 is compared with $B_{1,r_2} = [0\ \frac{T_s}{l_2}\ 0\ 0]^T$, the on-ramp-dependent column of B_1, it can be shown that the cell densities downstream of on-ramp inflow r_2 (ρ_2 through ρ_4) are controllable from r_2, whereas the upstream density (ρ_1) cannot be controlled from r_2. When the section is fully congested, the situation is reversed: ρ_1 is controllable from r_2, but the downstream states ρ_2 through ρ_4 are not controllable from r_2.

Generally, a section in free-flow mode is controllable from an on-ramp at its upstream end, whereas a congested section can be controlled from an on-ramp at its downstream end. If a section is in CF mode, it cannot be controlled by an on-ramp at either end of the section, while the opposite is true for the FC modes.

3 Results

Fig. 3 is a schematic diagram of the freeway section used to test both the modified cell transmission model and switching-mode model. It is a subsection of I-210 West, approximately 2 miles in length, with four

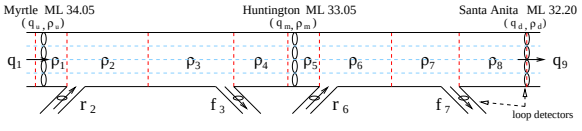

Figure 3: A segment of I-210W divided into cells

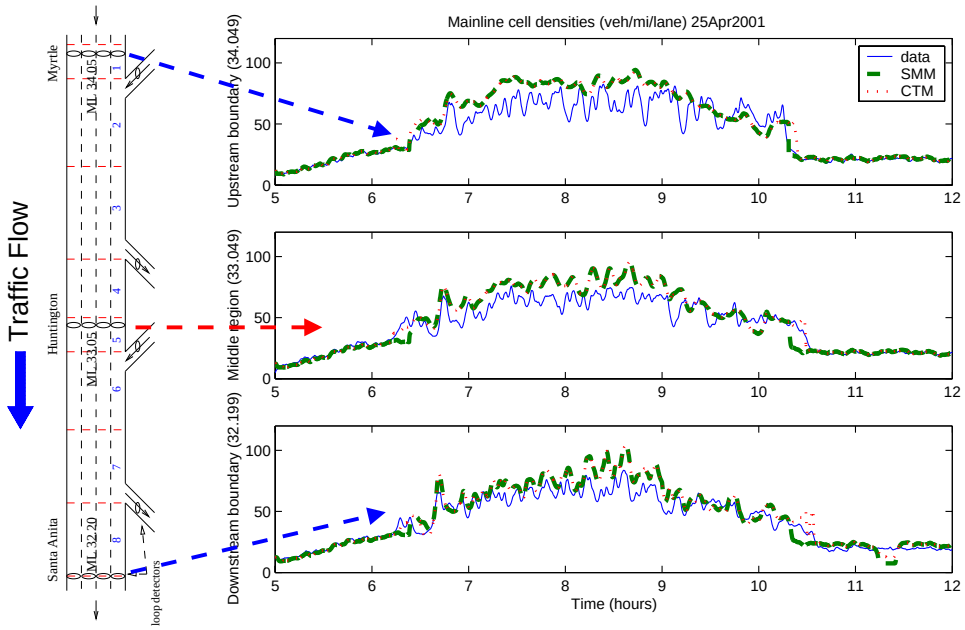

Figure 4: Measured and simulated mainline densities for a segment of I-210W on April 25, 2001

mainline lanes, three mainline loop detector stations labeled Myrtle (ML 34.05), Huntington (ML 33.05), Santa Anita (ML 32.20), and additional detector stations on each ramp. ML stands for "mainline", and the numbers, e.g. 34.05, are the absolute postmile indices of the detector stations (postmiles are a measurement of distance, in miles, along the highway). Fig. 3 shows the mainline segment partitioned into eight cells. The on-ramp flow into cell i is r_i, and f_j is the off-ramp flow exiting cell j. The mainline cell lengths chosen for the segment were $[0.088\ 0.375\ 0.375\ 0.192\ 0.088\ 0.276\ 0.276\ 0.246]$ mi.

We make several assumptions in order to relate the measured quantities ($q_u, \rho_u, q_m, \rho_m, q_d, \rho_d$, and flows measured at each on- and off-ramp) to flows and densities used by the model: (1) ρ_u is a measurement of the density in the first cell, i.e. $\rho_u = \rho_1$; (2) similarly, $\rho_d = \rho_8$; (3) the middle density ρ_m is a measurement of ρ_5, since the middle ML station (Huntington) lies within cell 5; (4) r_i (or f_j) is equal to the measured on-ramp (or off-ramp) flow at the corresponding on-ramp (or off-ramp) station.

The loop detector data used in this study was obtained from the Performance Measurement System (PeMS) [1]. Each loop detector provides measurements of volume (veh/timestep) and percent occupancy every 30 sec. In the case of the ML detectors, densities (veh/mi) can be computed for each lane using $\textit{density} = \frac{\textit{occupancy}}{\textit{g-factor}}$, where the *g-factor* is the effective vehicle length, in miles, for that detector. For single loop-detector freeways such as I-210, PeMS provides g-factors calculated according to the PeMS algorithm, described in [6].

A necessary condition for numerical stability is that vehicles traveling at the maximum speed may not cross multiple cells in one time step, that is, $vT_s \leq l_i$, $i = 1, 2, \ldots, N$. This, combined with the aforementioned cell lengths prohibits a simulation time step as large as 30 seconds, thus a zeroth-order interpolation was applied to the PeMS data to yield data with T_s = 5 sec. To counteract noise in the PeMS 30-sec data, a 1st-order Butterworth lowpass filter with cutoff frequency $.01T_s^{-1}$ Hz was applied to the data using a zero-phase forward-and-reverse filtering technique. One difficulty in selecting a test section is that it is rare for all the loop detectors in a section to be functioning properly at the same time. In the cases where detectors were not functional, the data was corrected using information from neighboring sensors. The interpolated, filtered, and corrected data sets were used as simulation inputs.

Several of the cell parameters used in these simulations (v = 63 mph, Q_M = 8000 veh/hr, ρ_J = 688 veh/mi) were estimated through a hand-tuning procedure, wherein Eq. (2) was evaluated over the 5AM–12PM time range using measured mainline densities in place of cell densities, with nominal values for v, w, and ρ_J. v, Q_M and ρ_J were subsequently adjusted to improve the agreement between the empirical evaluation of Eq. (2) and the measured mainline flows. w = 14.26 mph and ρ_c = 127 veh/mi were then computed as functions of the estimated v, Q_M, and ρ_J, assuming that all the parameters must satisfy the triangular fundamental diagram shape of Fig. 1. Since a flow-density hysteresis loop was often observed in the empirical flow vs. density plots, an approximate flow hysteresis was induced in the models by reducing w from 14.26 mph to 12.5 mph at 9AM. Spatially uniform parameters are a reasonable assumption for this freeway segment, which contains no abrupt varia-

Table 3: Mean percentage errors of ρ_5 estimates for several different days

Date	CTM	SMM
Mar. 15, 2001	0.117	0.129
Mar. 27, 2001	0.108	0.129
Apr. 02, 2001	0.109	0.125
Apr. 10, 2001	0.165	0.111
Apr. 25, 2001	0.126	0.142
mean	0.125	0.127
std. dev.	0.023	0.011

tions in geometry.

Both the switching model and modified CTM were simulated for the section of Fig. 3 using data collected from I-210 West for several weekdays, over the interval 5AM-12PM, during which the morning rush-hour congestion normally occurs. It was assumed that the upstream and downstream mainline data (q_u, ρ_u, q_d, ρ_d), as well as the ramp flow data, were known, whereas the middle density, ρ_m, was considered to be "missing", hence in need of estimation. The purpose of the test was to determine whether the models could accurately reproduce ρ_m.

Fig. 4 shows each of the three measured densities compared with its corresponding simulated density, for the cells nearest the ML stations, for a particular morning (4/25/01, 5AM–12PM). In the top graph, the measured upstream density, ρ_u, is plotted along with the simulated cell 1 density, ρ_1, for both the switching and modified cell transmission models. The cell 8 density, ρ_8, is compared with ρ_d in the bottom plot. Note that the simulated ρ_1 and ρ_8 are not identical to the nearby measured densities; this discrepancy between the model outputs and the "known" measurements ρ_u and ρ_d can be eliminated using an appropriate closed-loop estimation scheme. In the middle graph, ρ_m is plotted against the cell 5 density $\rho_5 = \hat{\rho}_m$. All the densities displayed in Fig. 4 were divided by the number of ML lanes.

Table 3 shows the mean-percentage error, defined as $E_{MPE} = \frac{1}{M}\sum_{k=1}^{M}\left|\frac{\rho_m(k)-\hat{\rho}_m(k)}{\rho_m(k)}\right|$, of each of the estimates for five different days in 2001. The mean error over the five days is approximately 13%. The results indicate that both the SMM and modified CTM provide a good estimate of ρ_m. As seen in Fig. 4 and Table 3, the performance of the two models is quite similar.

4 Conclusions and Future Work

The CTM-derived switching-mode model can be used as a freeway traffic density estimator. It is useful for determining the controllability and observability properties of the highway, which are of fundamental importance in the design of data estimators and ramp-metering control systems. We are currently working to extend the SMM-based data estimation methods to the remaining portions of I-210, and to perform more extensive testing to determine the best sets of parameters for the cell transmission and switching-mode models. Since off-ramp flow data for I-210 is generally incomplete or unavailable, we are currently developing a method, based on the switching-mode model, for estimating off-ramp flows. Additionally, we are investigating the switching-mode model as a basis for designing and testing new local ramp metering strategies. A hybrid system model closely related to the SMM has already been used to analyze the stability of local traffic responsive ramp metering controllers [7]. In addition to the design of controllers and estimators, fault detection and fault handling algorithms can be developed based on the SMM. This is important since data availability and data integrity are of great concern when implementing ramp metering control algorithms in the field.

Acknowledgments

The authors would like to thank Gabriel Gomes for his assistance in providing geometrical and time-series data for I-210.

References

[1] Freeway Performance Measurement Project. `http://pems.eecs.berkeley.edu/`.

[2] Markos Papageorgiou, H.S. Habib, and J.M. Blosseville. ALINEA: A Local Feedback Control Law for Onramp Metering. *Transportation Research Record*, 1320:58–64, 1991.

[3] Carlos F. Daganzo. The Cell Transmission Model: A Dynamic Representation of Highway Traffic Consistent with the Hydrodynamic Theory. *Transportation Research - B*, 28(4):269–287, 1994.

[4] Carlos F. Daganzo. The Cell Transmission Model, Part II: Network Traffic. *Transportation Research - B*, 29(2):79–93, 1995.

[5] Wei-Hua Lin and Dike Ahanotu. Validating the Basic Cell Transmission Model on a Single Freeway Link. PATH Technical Note 95-3, Institute of Transportation Studies, University of California at Berkeley, 1994.

[6] Zhanfeng Jia, Chao Chen, Ben Coifman, and Pravin Varaiya. The PeMS Algorithms for Accurate, Real-Time Estimates of g-factors and Speeds from Single-Loop Detectors. In *2001 IEEE Intelligent Transportation Systems Conference Proceedings*, pages 536–41, Oakland, CA, August 2001.

[7] Gabriel Gomes and Roberto Horowitz. A Study of Two Onramp Metering Schemes for Congested Freeways. In *2003 American Control Conference Proceedings*, Denver, CO, June 4–6 2003. to appear.